



Ultra-high-field 7T MRI in Parkinson's disease: ready for clinical use?—a narrative review

Thomas Welton^{1,2^}, Septian Hartono^{1,2,3}, Yao-Chia Shih^{2,3,4}, Stefan T. Schwarz^{5,6}, Yue Xing⁵, Eng-King Tan^{1,2}, Dorothee P. Auer^{5,7}, Noam Harel⁸, Ling-Ling Chan^{1,2,3^}

¹National Neuroscience Institute, Singapore, Singapore; ²Duke-NUS Medical School, Singapore, Singapore; ³Department of Diagnostic Radiology, Singapore General Hospital, Singapore, Singapore; ⁴Graduate Institute of Medicine, Yuan Ze University and National Taiwan University, Taipei; ⁵Mental Health and Clinical Neurosciences, School of Medicine, University of Nottingham, Nottingham, UK; ⁶Department of Radiology, Cardiff and Vale University Health Board, Cardiff, Wales, UK; ⁷NIHR Nottingham Biomedical Research Centre, University of Nottingham, Nottingham, UK; ⁸Center for Magnetic Resonance Research, University of Minnesota, Minneapolis, MN, USA

Contributions: (I) Conception and design: T Welton, EK Tan, DP Auer, N Harel, LL Chan; (II) Administrative support: None; (III) Provision of study materials or patients: None; (IV) Collection and assembly of data: T Welton, S Hartono; (V) Data analysis and interpretation: All authors; (VI) Manuscript writing: All authors; (VII) Final approval of manuscript: All authors.

Correspondence to: Dr. Ling-Ling Chan, MD. Department of Diagnostic Radiology, Singapore General Hospital, Block 2, Level 1, Singapore 169608, Singapore; National Neuroscience Institute, Singapore, Singapore; Duke-NUS Medical School, Singapore, Singapore. Email: chan.ling.ling@singhealth.com.sg.

Background and Objective: The maturation of ultra-high-field magnetic resonance imaging (MRI [≥ 7 Tesla (7T)]) has improved our capability to depict and characterise brain structures efficiently, with better signal-to-noise ratio (SNR) and spatial resolution. We evaluated whether these improvements benefit the clinical detection and management of Parkinson's disease (PD).

Methods: We performed a literature search in March 2023 in PubMed (MEDLINE), EMBASE and Google Scholar for articles on “7T MRI” AND “Parkinson*”, written in English, published between inception and 1st March, 2023, which we synthesised in narrative form.

Key Content and Findings: In deep-brain stimulation (DBS) surgical planning, early studies show that 7T MRI can distinguish anatomical substructures, and that this results in reduced adverse effects. In other areas, while there is strong evidence for improved accuracy and precision of 7T MRI-based measurements for PD, there is limited evidence for meaningful clinical translation. In particular, neuromelanin-iron complex quantification and visualisation in midbrain nuclei is enhanced, enabling depiction of nigrosomes 1–5, improved morphometry and vastly improved radiological assessments; however, studies on the related clinical outcomes, diagnosis, subtyping, differentiation of atypical parkinsonisms, and monitoring of treatment response using 7T MRI are lacking. Moreover, improvements in clinical utility must be great enough to justify the additional costs.

Conclusions: Together, current evidence supports feasible future clinical implementation of 7T MRI for PD. Future impacts to clinical decision making for diagnosis, differentiation, and monitoring of progression or treatment response are likely; however, to achieve this, further longitudinal studies using 7T MRI are needed in prodromal, early-stage PD and parkinsonism cohorts focusing on clinical translational potential.

Keywords: Parkinson's disease (PD); magnetic resonance imaging (MRI); ultra-high field strength; 7 Tesla (7T)

[^] ORCID: Thomas Welton, 0000-0002-9503-2093; Ling-Ling Chan, 0000-0001-7603-7334.

Submitted Apr 26, 2023. Accepted for publication Sep 15, 2023. Published online Oct 17, 2023.

doi: 10.21037/qims-23-509

View this article at: <https://dx.doi.org/10.21037/qims-23-509>

Introduction

Ultra-high-field magnetic resonance imaging (MRI) [≥ 7 Tesla (7T)] technology has been used in basic science and neuroscience applications for the past two decades (1,2) and, in recent years, has been maturing for clinical applications, with increased performance and availability. The greater signal-to-noise ratio (SNR) and contrast-to-noise ratio (CNR) of 7T MRI offer better resolution, contrast and speed, improving our capability to depict and characterise brain structures efficiently (3,4). With the U.S. Food and Drug Administration (FDA) approval of new 7T platforms in 2020, this will likely increase the usage of 7T MRI in radiology clinics and for research in the coming years. There are presently (early 2023) more than 90 7T MRI installations worldwide.

With increasingly aged and multi-morbid populations, the prevalence of Parkinson's disease (PD), currently >10 million worldwide, is expected to double over the next 30 years (5). Major clinical challenges include uncertainty in diagnosis in early or suspected PD, differentiation of PD from atypical parkinsonisms, accuracy and side effects in deep-brain stimulation (DBS) surgery, and measurement of neuropathology to monitor treatment response or progression.

Recent studies have applied 7T MRI in PD using a range of imaging sequences, showing evidence for better visualisation (6), more accurate quantitative biomarkers (7), and improved stratification (8). However, a better understanding is needed of how and why these direct improvements to accuracy and detail of the measurement of PD-relevant pathology could meaningfully impact clinical decision making. Reviews have included 7T MRI of PD as (part of) their scope (9,10), but the literature lacks a focused and comprehensive review on the topic that includes recently-published articles (including and since 2021). Moreover, previous reviews have not integrated knowledge from clinical 7T MRI studies to discuss the potential role of 7T MRI in a clinical workflow, or the possible impact on clinical decision making.

This review does not aim to make direct comparison between 3T and 7T MRI. This is due to their contrasting roles in clinical practice. While 3 Tesla (3T) MRI is the

platform for routine clinical imaging, 7T is most often used as a problem-solving tool for difficult cases, taking a complementary but different position alongside (not replacing) existing MRI machines. A fair comparison is further complicated by decades of optimisation at 3T.

In this narrative review, we ask, "What is the potential for ultra-high field MRI to improve clinical decision making for PD?". We review (I) the relevance of recent advances and challenges in 7T MRI technology to PD, (II) the existing evidence from studies that have applied 7T MRI in PD, and (III) how and why the recent advances at 7T could benefit clinical decision-making for PD. We present this article in accordance with the Narrative Review reporting checklist (available at <https://qims.amegroups.com/article/view/10.21037/qims-23-509/rc>).

Methods

The search strategy and methods are reported in *Table 1*. We identified a total of 307 articles.

Technological advances at 7T and relevance for PD

The conventional clinical role of MRI at 1.5T or 3T for PD is currently limited to investigating (I) loss of the "swallow-tail" radiological sign from susceptibility-weighted imaging (SWI) (11), indicating nigrosome-1 (N1) degeneration, and (II) DBS surgical planning. For general technological advances of 7T, we refer to recent reviews (12-14). In short, the increased magnetic field strength confers a better trade-off between SNR, spatial resolution, temporal resolution [for echo-planar imaging (EPI) sequences] contrast or other characteristics depending on the optimisation of the imaging sequence (4) that may yield benefits specifically for investigation of PD (15) (*Figure 1*). The increased field strength of 7T also brings additional challenges (12,17), including inhomogeneity of the B_0 field, gradient field (B_1) inhomogeneity, reduced penetration of radiofrequency (RF) through tissue, off-resonance image artefacts secondary to modulation of the RF phase and amplitude, motion artefacts, and safety (18).

In PD, loss of neurons in the lateral substantia nigra (SN) is the primary pathological hallmark. The presence of

Table 1 The search strategy summary

Items	Specification
Date of search	1st March 2023
Databases and other sources searched	PubMed (MEDLINE), EMBASE, Google Scholar
Search terms used	“7T MRI” AND “Parkinson*”
Timeframe	Inception to 1st March 2023
Inclusion and exclusion criteria	English language
Selection process	Selection conducted by Welton T based on titles and abstracts of articles

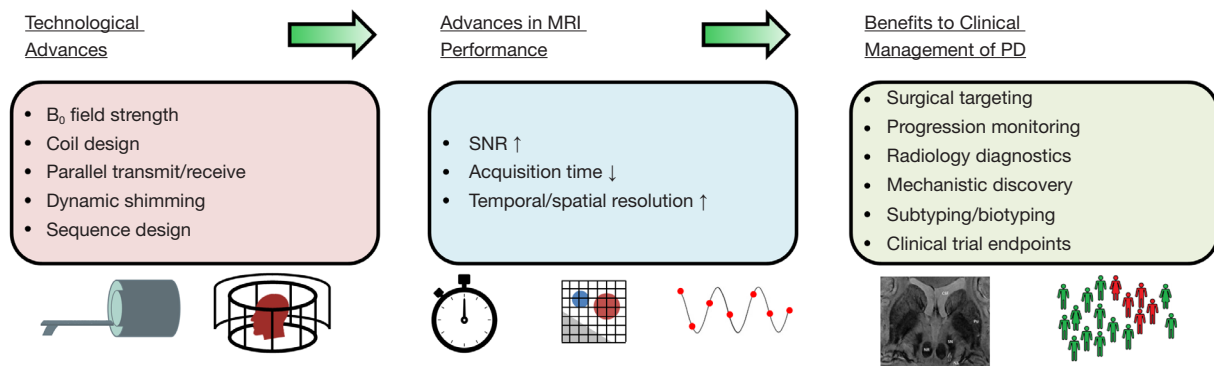


Figure 1 Overview of 7T MRI advances and benefits to PD imaging. The MRI image (right) was reproduced as-is, and was originally published under the Creative Commons Attribution 4.0 International (CC BY) license [Gramsch *et al.* 2017 (16)]. MRI, magnetic resonance imaging; SNR, signal to noise ratio; PD, Parkinson’s disease; 7T, 7 Tesla.

iron and its disruption of the local field homogeneity results in a lower T2 signal by reducing the transverse relaxation time. Thus, imaging tests in PD have aimed to visualise this region and to quantify neuromelanin-iron characteristics of a healthy SN. The healthy “swallow-tail” radiological sign occurs because the SN is rich in iron while N1 has relatively less iron, thus producing an image contrast. Loss of the swallow-tail sign occurs when degeneration of the N1 causes iron deposition and thus lessens the SN-N1 contrast. Loss of this sign in PD has been described (11) and can be visualised using magnetic susceptibility-sensitive sequences capable of detecting iron concentration (Figure 2, SN and N1). Therefore, of high relevance to PD at 7T is the improvement in SNR for T2*-weighted or SWI. This could obviate further image post-processing, as required on 3T, to reliably visualise the “swallow-tail” or confirm its loss (20).

SWI exploits the difference in magnetic susceptibility between tissues to create its image contrast. SWI suffers minimally from the challenges associated with 7T [i.e., increased radiofrequency field (B_1) inhomogeneity and

higher specific absorption rate (SAR) of radiofrequency energy]. For PD, SWI has been used in research to detect increased iron deposition in the deep brain nuclei. Quantitative susceptibility mapping (QSM) applies post-processing to allow quantification of the underlying magnetic susceptibilities, and has thus also found utility in PD for imaging the SN (21).

The pathophysiology of PD involves small nuclei, such as the SN and subthalamic nucleus (STN; Figure 2). At 7T, small structures can be better-resolved due to the possibility for higher spatial resolutions, and greater contrast (22). For example, at 3T, a routine structural neuroimaging sequence has a typical in-plane spatial resolution of 1 mm², compared to its equivalent of 0.8 mm² at 7T, or even up to 0.25 mm² by limiting coverage (Table 2). Better spatial resolution reduces partial volume effects, and improves qualitative assessment and segmentation precision, including that by automated software. More precise volume and shape estimates translate into more objective and accurate quantitative measurements (23).

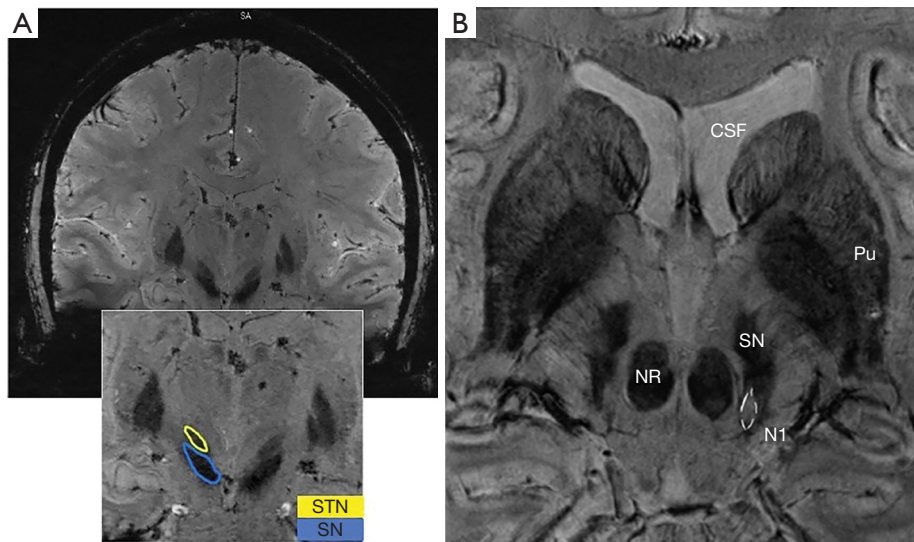


Figure 2 Examples of susceptibility-weighted images gathered at 7T. (A) Shows the STN (yellow) and SN (blue) in a coronal slice from a SWI image at 7T. 7T allows clear segmentation of these structures which is normally not possible at 3T without further image postprocessing, and is useful when planning deep-brain stimulation surgery. (B) Shows a narrower field of view axial slice through the basal ganglia from a 7T SWI image, demonstrating intra- and inter-nuclear differences in texture and contrast in e.g., Pu, SN, NR and N1 as compared to CSF. Both subfigures, (A,B), were reproduced as-is, and were originally published under the Creative Commons Attribution 4.0 International (CC BY) license. Subfigure (A) was *Fig. 1* from Duchin *et al.* 2018 (19), and subfigure (B) was *Fig. 1* from Gramsch *et al.* 2017 (16). STN, subthalamic nucleus; SN, substantia nigra; CSF, cerebrospinal fluid; Pu, putamen; NR, nucleus ruber/red nucleus; N1, nigrosome 1; SWI, susceptibility weighted imaging; 7T, 7 Tesla.

Table 2 Example useful clinical MRI sequences for Parkinson's disease at 7T

Parameter	3D T1 MPRAGE	FLAIR TSE 2D	T2* GRE
Voxel dimensions (mm)	0.8×0.8	0.7×0.7	0.3×0.3
Matrix size	300×320	240×320	520×640
No. slices	190	35	96
Field of view (mm)	225×240	175×230	169×208
Slice thickness (mm)	0.8	3	1.2
TE (ms)	4.15	125	15
TI (ms)	2,600	–	–
TR (ms)	5,000	9,000	27
Acquisition time (min:s)	8:00	4:00	5:00
GRAPPA factor	3	2	3
Bandwidth (Hz/pixel)	180	244	140
FA (°)	4	180	15

These approximate protocols are a guide and real implementations will vary depending on many factors including the specific hardware used. MRI, magnetic resonance imaging; 7T, 7 Tesla; 3D T1 MPRAGE, 3-dimensional T1-weighted magnetization-prepared rapid acquisition gradient echo; FLAIR TSE 2D, fluid-attenuated inversion recovery turbo spin echo 2-dimensional; T2* GRE, T2*-weighted gradient recalled echo; TE, echo time; TI, inversion time; TR, repetition time; GRAPPA, generalized autocalibrating partial parallel acquisition; FA, flip angle.

Research studies in PD have identified a number of changes to brain network connectivity using functional MRI (fMRI) and diffusion-tensor imaging (DTI) techniques (24,25). A key parameter in these sequences is the temporal resolution, which describes the number of repeated images gathered within a given time. At higher temporal resolutions, the effects of aliasing (incorrect measurement of frequency due to low sampling rate) are reduced. Additionally, physiological noise can be more effectively accounted for in post-processing when images are acquired faster. However, some scan parameters should be determined based on the tissue relaxation times (e.g., repetition time and flip angle) and so are affected by the shorter longitudinal relaxation time at 7T. Secondly, SNR would decrease as temporal resolution increases so, while temporal resolutions can be vastly increased at 7T, the optimal value for this parameter should be chosen carefully.

Evidence from clinical studies

Quantification and visualisation of iron content

Loss of neurons in the SN in PD occurs simultaneously with changes in iron homeostasis, and various MRI parameters have been used to quantify this change.

The first such study at 7T quantified magnetic susceptibility in the SN, showing a significant difference between PD patients and controls in the pars compacta, but not the whole SN (26). 3D renderings of susceptibility across the SN showed variation with great detail. Post-mortem 7T imaging using various MRI parameters could delineate the spatial distributions of the neuromelanin-iron complex and ferric iron within the SN and was validated using histology (27). This demonstrated a capability to differentiate the two, which could be useful for evaluating progression of iron distribution in PD. The same group later tested their approach, based on the mismatch between T2 and T2* relaxation times, in post-mortem brains of PD patients, as well as the feasibility of measuring neuromelanin *in vivo* (6). The dorsal SN pars compacta had mismatch between T2 and T2* in healthy subjects corresponding to neuromelanin distribution, as confirmed by histology. In the depigmented SN, no such pattern or mismatching was observed. 7T MRI was also able to detect signal changes in nigrosomes 2–5 (Figure 3), albeit with less confidence than for N1, which had the largest signal reduction (16,22). More recently, neuromelanin-related markers evaluated at 7T showed a 50% reduction in CNR of magnetisation-

transfer imaging in PD compared to controls and a 1.2-fold increase in ferric iron loading (7). Other studies at 7T have used QSM, for example showing superior CNR and improved visualisation of the STN for QSM than T2*-weighted MRI (30) and secondly to quantify SN volume loss (8).

Advanced imaging with magnetic susceptibility based techniques at 7T therefore has a proven capability to depict the SN in greater detail than at 3T (28) and to detect iron homeostatic changes (Figure 3B). By highlighting the deep complexity of the SN and its iron properties, further questions are raised: the SN is increasingly regarded as a complex structure comprising a rich array of small substructures which, themselves, vary in composition, role, and clinical relevance. Furthermore, the iron content itself can be further subdivided into ferric or neuromelanin-bound iron. It is not yet known which susceptibility-based measures might be most useful for PD clinical management.

Radiological assessment

Others have attempted to use 7T MRI in radiological studies of PD, to test diagnostic performance and ability to qualitatively delineate relevant brain structures.

For example, 7T and 3T T2*-weighted images were examined by a neuroradiologist to detect the presence or absence of N1 (visualised as a hyperintense ovoid substructure within the dorsal/posterior hypointense midbrain region; Figures 2,4) (31). Both *in-vivo* and post-mortem MRIs could directly visualise the loss of the N1 substructure, and this was verified by histology in the post-mortem brains. N1 was better visualised at 7T than 3T. Two radiologists were able to distinguish 17 PD patients from 13 healthy subjects based on the appearance of the SN in 7T SWI images alone with good sensitivity (100%) and specificity (96.2%) (32). They classified the SN as abnormal if a three-layered organisation or hyperintense lateral spot was not visible in the more rostral SN, or if there was no hyperintensity in both the medial and lateral parts of the caudal SN. Figure 4 shows examples of healthy and PD SN/N1.

In another study, combined gradient and spin-echo (GRASE) and 3D gradient echo sequences were compared at 7T in terms of the CNR in midbrain nuclei (33), with both showing good visible contrast for anatomic delineation including minute vascular contrast between SN subregions. The addition of spin echoes in the GRASE sequence helped to increase CNR. Susceptibility-weighted angiography (SWAN) was performed at 7T and compared to 3T on

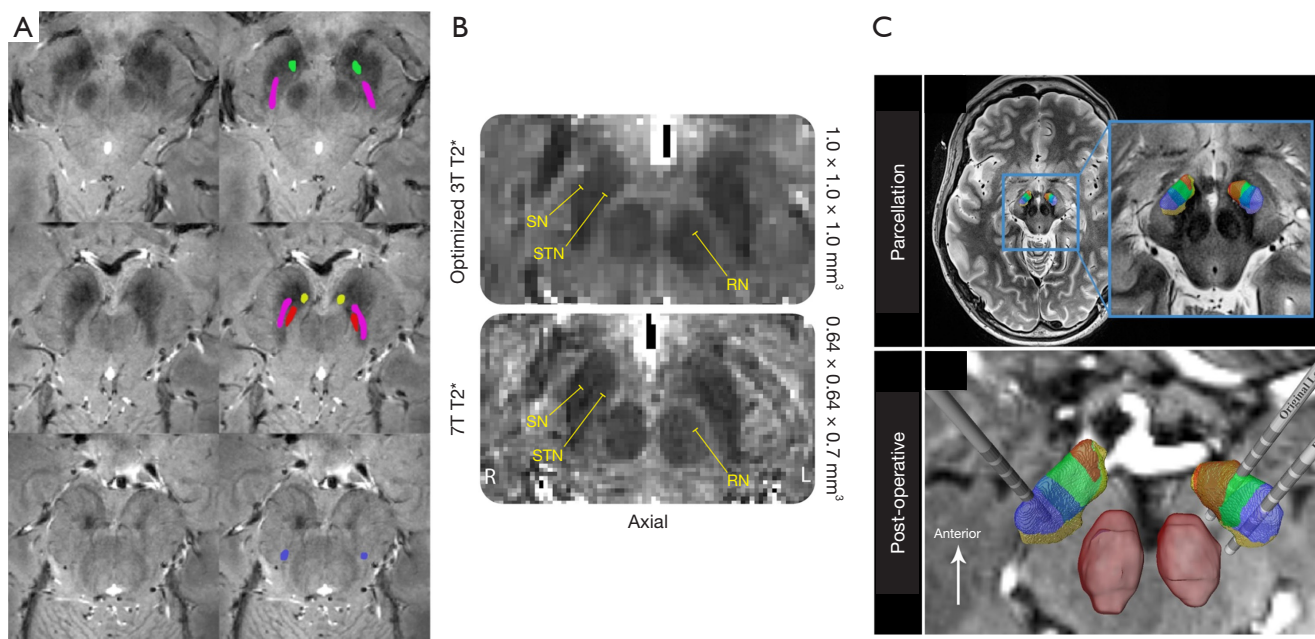


Figure 3 Results from recent clinical studies applying 7T MRI in Parkinson's disease. (A) T2*-weighted 7T MRI visualisation of nigrosomes 1–5 in a 60-year-old Parkinson's disease patient from the rostral, medial and caudal substantia nigra (top, middle, bottom rows) with N1 = purple, N2 = yellow, N3 = blue, N4 = red and N5 = green. (B) Comparison of 3T and 7T MRI T2*-weighted images, showing superior resolution and visualisation of substructures at 7T. (C) DBS implantation in a 52-year-old with Parkinson's disease showing that sub-parcellation of the subthalamic nucleus (multi-coloured) and red nucleus (red) could assist in repositioning of original (incorrect) lead location to the sensorimotor region (blue). Subfigures (A–C) were adapted from their original published versions (cropped), and were originally published under the Creative Commons Attribution 4.0 International (CC BY) license. Subfigure (A) was adapted from Fig. 1 by Schwarz *et al.* 2018 (22), subfigure (B) was adapted from Fig. 2 by Isaacs *et al.* 2020 (28), and subfigure (C) was adapted from Fig. 1 by Schrock *et al.* 2021 (29). 7T, 7 Tesla; 3T, 3 Tesla; STN, subthalamic nucleus; SN, substantia nigra; RN, red nucleus; MRI, magnetic resonance imaging; DBS, deep-brain stimulation.

radiologist assessment for SN abnormalities (34). PD could be diagnosed using the 7T images with an accuracy of 96% (in 14 patients *vs.* 13 controls), and at 3T with 86% accuracy. Another study further demonstrated the improved qualitative assessment of structures at 7T (35). Finally, magnetisation-transfer imaging of the locus coeruleus (LC) at 7T has been proposed as a method to aid in PD diagnostics (36). Magnetisation-transfer effects underlie the contrast in the LC and can be detected at high resolution using 7T MRI, which was superior to the conventional 2D T1-weighted turbo spin echo sequence commonly used to image the LC (36). Furthermore, magnetisation contrast in the LC correlated with measures of cognition and apathy at 7T in PD patients (37), while other early studies have explored the optimal LC imaging contrast (38) and structural connectivity of the LC (39) utilising 7T MRI data.

The Swallow-Tail radiological sign (11) was evaluated for reliability and consistency at 7T, and it was found that it could be reliably detected (40). The increased performance of 7T MRI was able to tease-out the further possibility that the sign is individually variable in healthy individuals due to the normal variation in N1 molecular organisation.

These studies together demonstrate the capability of 7T MRI to not only depict the outline and shape of the whole SN (Figure 4), but also its inner organisation (pars reticulata, dorsal and ventral pars compacta), contributing to an improved radiological assessment and diagnosis of PD based on MRI, and use of radiological signs to almost perfectly discriminate PD from controls in some instances. Such data may eventually reduce the need for expensive and irradiating dopamine transporter (DAT) scans. The usefulness of 7T in detecting early or prodromal signs of PD is not yet known.

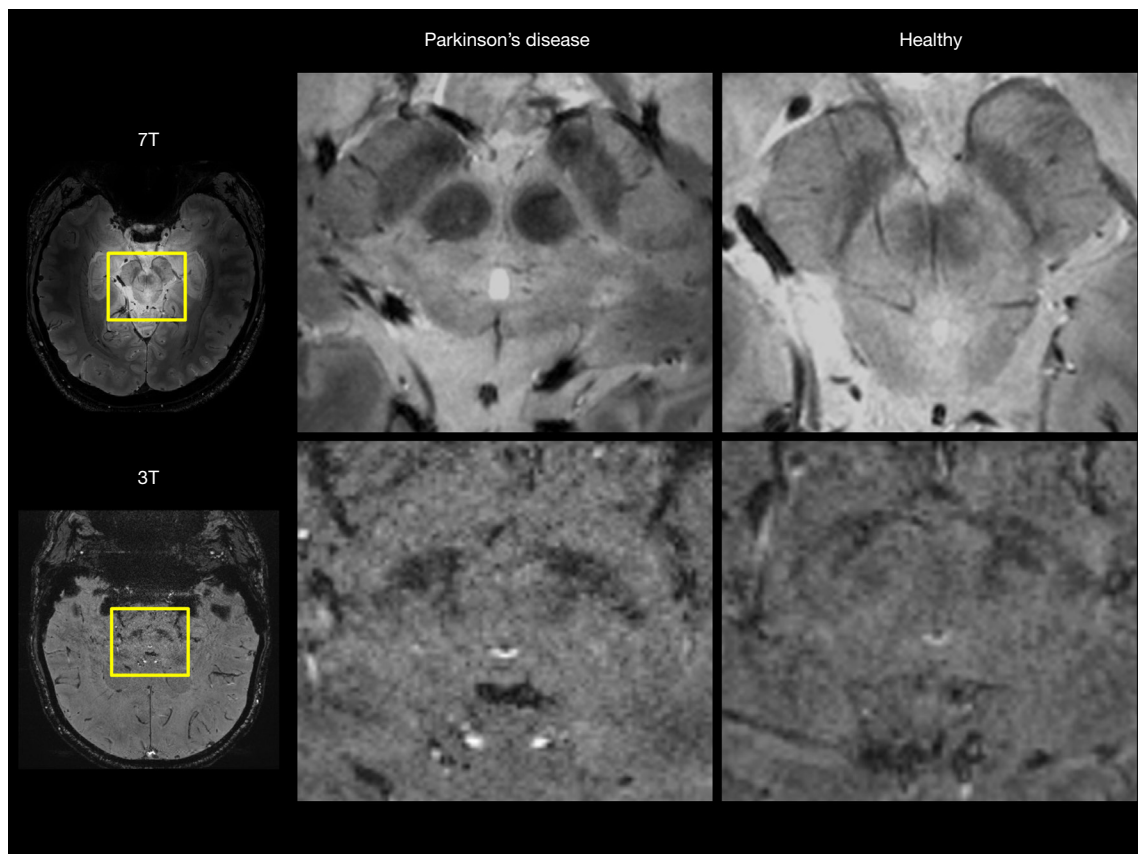


Figure 4 Comparison of midbrain T2*-weighted images between Parkinson's disease and healthy individuals at 7T and 3T. The swallow-tail sign is visible in the healthy subject for both field strengths. The shape and size of both substantia nigra and nigrosome 1 can be more readily delineated at 7T. The red nucleus is visible in the 7T images because they were acquired along the anterior commissure-posterior commissure line, while the 3T images were acquired slightly more oblique to coronal. T2*-weighted 7T images were acquired on a 7T Philips Achieva using 32-channel receiver coil (2D fast-field echo sequence with TE/TR =16/412 ms, FA =40°, no sense, 2 signal averages, FOV =180 mm × 160 mm × 16 mm, and 0.35 mm × 0.35 mm × 1 mm resolution in 9.5 minutes). 3D T2* SWI multi-echo gradient echo sequence was acquired on a 3T Siemens Skyra using 32-channel receiver coil (TR =48 ms, TE =13.77/26.39/39 ms, FA =20°, FOV =192 mm × 192 mm × 32 mm, and 0.5 mm × 0.5 mm × 1 mm resolution in 4.25 minutes). 7T, 7 Tesla; 3T, 3 Tesla; TE, echo time; TR, repetition time; FA, flip angle; FOV, field of view; SWI, susceptibility weighted imaging.

Morphometry

Several studies measured the volumes of the SN and other regions implicated in PD, noting consistent reductions in volume in PD versus controls and remarking on the advantages of 7T structural imaging in contrast and spatial resolution for volumetrics (8,23,33,41-44). Studies of atrophy have not been confined to the midbrain nuclei, as a global cortical reduction has also recently been found using 7T, with predominance in prefrontal and hippocampal regions (45). The clinical utility of 7T for the purpose of improved atrophy measurements may be limited, since

atrophy is prominent in later stages of PD. On the other hand, brain atrophy patterns in PD appear to have distinct subtypes (46), which could hint at variation in underlying aetiology, and 7T MRI could identify these with greater detail and accuracy.

Others have attempted to parameterize the shape of the SN, taking advantage of higher spatial resolution to measure differences in the smoothness of the lateral SN surface. Using a T2*-weighted sequence at 7T with 0.25 mm² voxel size, an early study demonstrated the clear delineation of shapes and boundaries of the SN (42). The authors noted the arch-shaped boundary between the SN and crus cerebri

in normal controls, and devised a shape-based marker using the distance from the midline of the SN to the lateral boundary of the SN. This arch shape was blurred and deformed in PD patients, presumably due to the release of neuromelanin into adjacent tissue with degeneration. A second study by the same team gathered 3D T2*-weighted images to also investigate the undulation of the lateral SN surface (43). In a more sophisticated three-dimensional approach to shape analysis, the authors reconstructed the surface mesh of the SN [and other nuclei (35)] in minute detail. They showed that the rostral part of the SN lateral surface was inflected in PD patients, and more so in patients with more severe symptoms. Similarly, one study evaluated a metric based on relaxometry values in the SN, showing that PD patients had a smaller mismatching area (6).

Albeit in small samples, with few direct comparisons to lower field strengths, these studies demonstrate the potential for morphological measurements gathered at 7T to distinguish PD patients from controls based on the shape of anatomical structures. Further morphological studies at 7T are needed to understand how it may be used for subtyping.

DBS surgical targeting

7T MRI has been applied to enhance the imaging of anatomy for DBS, to minimise error in planning the initial trajectory, and to minimise adverse effects by interference with adjacent structures. Precision of DBS stimulation is critical since, even within the STN, the placement of the DBS lead has a significant impact on patient outcomes (47).

In a first example, SWI, T2-weighted and T1-weighted imaging were used to segment and visualise the globus pallidus, red nucleus, SN and STN at both 3T and 7T (35). Substructures, such as the ventral intermediate nucleus, were detected and readily distinguished with greater clarity, and this capability was proposed to enhance the targeting for DBS surgery. An important study by Duchin *et al.* (19) was the first to demonstrate the power of 7T for creating a true patient-specific anatomical model for pre- and post-DBS-surgery, with microelectrode validation. A later study used 7T MRI in 20 patients who underwent DBS to test whether the better morphological assessment could help improve electrode placement (48). Fusion of images from pre-operation (T1- and T2-weighted) with post-operative computed tomography (CT) scan was used to develop an interactive report with precise 3D visualisation of the electrode placement in relation to key structures. More

fine-grained atlases of the globus pallidus and thalamus have been created using 7T MRI to aid in DBS targeting (49). More refined positioning could be achieved based on the connectomic properties of the region (29), for example in the STN and its subregional connectivity to motor regions versus associative, limbic or other regions (44). Clinical outcomes from DBS surgery with 7T-supported lead placement show clear improvement when patient-specific anatomical targeting is used (29) (*Figure 3C*). In this case report, a PD patient with an implanted DBS lead experienced severe mood side effects and little improvement in motor symptoms, which were resolved by precise repositioning of the lead from the limbic to the sensorimotor area of the STN (29). In this case, 7T MRI was instrumental in creating a personalised detailed map of STN connectivity and DBS lead targeting (29). In this patient, the motor symptom severity was improved by 71% within 16 weeks of lead repositioning and complete resolution of mood symptoms (29). Larger longitudinal studies which follow up after DBS, and use a patient-specific anatomical model for lead placement are needed.

Atlases and segmentation tools

The improved capability of 7T MRI to depict small nuclei has been used to create intricate new atlases of PD-related brain regions (44,49). For example, studies mapped the mesopontine tegmental nuclei (cuneiform, pedunculotegmental, oral pontine reticular, paramedian raphe and caudal linear raphe) (50) and the STN (51), which are involved in motor function and affected in PD and other movement disorders. The authors created and validated a stereotactic probabilistic template in a standardised space of these nuclei using T2-weighted and fractional-anisotropy images at 7T, which previously was not possible at lower field strengths. Another study created an atlas of the LC, which has severe cell loss in PD, using a combination of T1-weighted and magnetisation-transfer imaging (52). The authors achieved a precise localisation across their sample, which is notable due to the small size of the LC in cross-section (~2 mm). Such atlases could be useful in other research studies at lower field strengths using a range of imaging modalities to identify and segment regions with greater precision and confidence. On the other hand, one strength of 7T MRI is that it allows the construction of patient-specific models of anatomy (19), removing the need for averaging of multiple images to create atlases, which has previously been required due to

low SNR/CNR.

Functional and diffusion-based structural connectivity

Structural and functional connectomic analysis using diffusion MRI is enhanced at 7T by greater possible angular/temporal resolution and greater SNR, which could help to better understand the mechanisms of affected regions in PD, and to aid in visualisation of important tracts for surgical planning.

One such study probabilistically mapped the connections of the basal ganglia *in vivo* using 7T diffusion MRI (41). Detailed reconstructions of pathways among the basal ganglia were possible, including for the SN and STN, and compared to fMRI functional connectivity data for the same regions. The functional territories (subregions) of the STN (44) and globus pallidus (49) have also been mapped using diffusion MRI connectomics at 7T (49). Diffusion MRI has also been applied at 7T to show differences even in small regions in fractional anisotropy, for example, of the STN in PD (23).

The enhanced capabilities of 7T MRI could therefore enable connectomic measurements with potential application for personalised brain mapping (53). However, 7T MRI implementations of diffusion MRI have faced challenges which still limit its usefulness; in particular, the SAR is increased by employment of slice acceleration techniques, B_0 inhomogeneities, and inhomogeneity of flip angle throughout the brain which lowers the SNR in peripheral brain regions like the cerebellum and inferior temporal lobes (54).

Subtyping and evaluation of atypical parkinsonisms

A pilot study at 7T showed nigral involvement in atypical parkinsonisms (55). By visual assessment of SWAN images, readers correctly rated all controls as normal and found that 80% of patients had bilateral SN abnormalities [including patients with multiple system atrophy (MSA) and progressive supranuclear palsy (PSP)]. A further study in 26 patients (7 MSA and 3 PSP) and 30 controls also demonstrated the loss of N1 hyperintensity (56). Using SN volumes measured using 7T QSM, one study found differences between patient groups with bradykinesia/rigidity and tremor (8). Finally, rapid eye movement sleep behaviour disorder (RBD), which is a strong predictor of synuclein pathology, has been studied at 7T using SWI of the SN, which was abnormal in the majority of RBD patients and had high agreement with dopamine transporter (DAT) imaging (57).

Role in clinical workflow

Clinically, 7T MRI is a tool for resolving difficult cases or for research, taking an auxiliary position alongside existing MRI machines, rather than replacing them. PD referrals for 7T are clinically germane but not regarded as cost-efficient given the greater costs of infrastructure, labour, radiological reporting and mismatch in reimbursements. In a modified clinical imaging workflow, cases can be prioritised into 7T based on difficulty, characteristics of the case, and availability. The 7T MRI data should be supplemented by post-processing steps to provide additional value; for example, segmentations and fibre tracking for DBS candidates. New artificial intelligence (AI) tools could facilitate filtering of cases based on automatic detection of overt swallowtail sign loss at 3T (58).

Impact on clinical decision making

Diagnosis

One clinical issue that 7T MRI could help to address is uncertainty in diagnosis of suspected or early PD. In theory, improved imaging capability could allow radiologist assessment or quantitative biomarkers that have sufficient sensitivity and specificity to be clinically useful. Diagnostic performance must be considered through the lens of PD duration and severity, from pre-symptomatic, to prodromal, early, and late stages. The earlier in the disease process, the lower the sensitivity and specificity of classification based on changes in the neuromelanin-iron complex will be. Thus, importantly, current evidence for classification performance in diagnosed patients does not yet support classification performance in earlier stages.

None of the studies reviewed above provide evidence of diagnostic performance in pre-symptomatic, prodromal or early PD and have, so far, been limited in sample size while only reporting data for patients with established PD diagnoses. It may be that 7T MRI is not able to effectively diagnose PD in such patients, or due to the early state of the field or difficulties in acquiring such data. Nonetheless, there is no direct evidence currently showing that the improved image quality of 7T MRI improves the detection of PD before a diagnosis has already been made. To support this, sufficiently powered longitudinal studies are needed; to compare the suspected/pre-symptomatic phase MRI results against later-confirmed reference standard diagnoses.

On the other hand, evidence from diagnostic utility studies of PD patients with confirmed diagnoses shows good performance and improvements over 3T MRI (32,34).

Therefore, two key questions are (I) “how far along the spectrum of disease severity does this capability extend with clinically useful performance?” and (II) “how certain are the results in confirmed PD from a limited set of studies with limited sample sizes?”.

Subtyping and differential diagnosis of parkinsonisms

A related clinical challenge is uncertainty in differentiating PD from various forms of Parkinsonism. 7T MRI might provide new or improved radiological or quantitative assessments that are able to distinguish between PD and parkinsonisms, or subtypes of PD. Since atypical parkinsonism diagnosis and PD subtypes are determined on clinical grounds, then, in order to be useful, a 7T MRI must be able to either increase the confidence of this diagnosis or be able to predict it in advance.

The few published studies at 7T in this area (8,55,56) do not show evidence of either increased confidence or prediction. Furthermore, studies at lower field strengths are still unclear whether MRI can distinguish parkinsonisms, so further work is needed and currently clinical decision making in this area is not impacted by 7T MRI.

DBS surgery

It is imperative in DBS surgery that the imaging used during planning is accurate to avoid adverse effects and maximise the treatment efficacy. While MRI is used to determine the locations of key structures and the initial trajectory for the electrode, the final placement is usually determined by intraoperative microelectrode recording and test stimulations. As such, potential roles for 7T MRI in DBS surgery are in minimising error in the initial trajectory and limiting adverse effects by interference with important tracts and structures.

Current evidence suggests that, indeed, clinical outcomes can be improved and adverse effects reduced by 7T MRI-guided DBS surgery, although more evidence with larger samples is needed in this area (29), and longitudinal studies are needed to compare the long-term outcomes from surgeries planned with 7T MRI versus those planned with 3T MRI.

Monitoring neuropathology for progression and treatment response

Another clinical challenge is to determine the most effective

PD treatments. Alongside conventional symptomatic improvement outcomes, clinical trials of PD treatments often aim to measure MRI-based markers as secondary outcomes. It is imperative in clinical trials to have accurate and precise outcome measures to (I) most effectively determine the treatment effect and (II) to understand the neuropathological response. 7T MRI may address this by providing more accurate biomarkers that link closely to pathophysiology. Secondly, with improved tools, it may be possible to measure neuropathological treatment effects on an individual basis to examine a patient’s response to new medication and determine the appropriate course of action. It may be that a neuropathological response occurs before symptomatic improvement manifests. In both applications, quantitative MRI based measures could feasibly be useful, but should improve on existing tools, like reduced dopaminergic activity in the putamen measured with ¹⁸F-fluoro-3,4-dihydroxyphenylalanine positron emission tomography.

Studies at 7T MRI have proposed a host of new measurements for quantifying iron content and morphology of the SN. They also show that 7T MRI out-performs 3T MRI in terms of accuracy and precision. However, whether these improvements impact clinical decision making has not been sufficiently investigated. Studies are needed that compare 7T MRI-based quantitative measures with blood- and tissue-based measures of pathology, to show whether a tangible benefit is gained from this increased accuracy/precision. If so, this may impact the selection of quantitative measurements for neuropathological monitoring, such as for clinical trial outcomes.

Strengths and limitations

A strength of this work is that it is presently the most up-to-date and comprehensive review to our knowledge on 7T MRI in PD, covering all relevant technologies and applications. A limitation is that we could not provide sufficient estimates of costs for 7T MRI, which may have been useful to prospective institutions; this was due to geographic variation and variation in cost structure. As a narrative review, we did not systematically include and evaluate all literature pertaining to this topic. Narrative reviews may be prone to selection bias, but we have attempted to provide a fair and balanced interpretation. On the other hand, this allowed more opportunity to contribute our insight and speculate on the possibilities for 7T MRI in PD.

Knowledge gaps and future work

There is a breadth of potential applications for 7T MRI in PD (Appendix 1). Future research should focus on showing how the clearly existing improvements in image quality at 7T can gain meaningful clinical translation into the radiological workflow and therapeutic trials. Surgical targeting studies using 7T MRI require long-term follow-up to evaluate the success rate, and frequency of adverse effects. Subtyping studies should make use of enhanced imaging and machine learning capabilities to (I) classify patients into *de novo* clinical subtypes and (II) use data-driven approaches to identify new subtypes. Identification of quantitative biomarkers based on iron content is a further area for exploration, for example in prodromal PD and in the subnuclei, such as N1 versus nigrosomes 4 or 2 (59,60). There is a lack of clinical studies directly comparing 3T MRI with 7T MRI, which limits a true clinical evaluation. One noteworthy on-going longitudinal study is gathering 7T MRI, genetic, motor, cognitive and neuropsychiatric data on PD patients (61). There is a need for standardised 7T imaging protocols for PD and establishment of working groups to design and implement them. Finally, this area will need more studies on feasibility and patient perspectives to move forward with adoption. Once these are better supported, a long-term goal should be to determine whether the improvements to clinical outcome justify the additional costs.

Conclusions

Our review of technical advances and challenges for 7T MRI in PD shows that there are clear theoretic benefits available—some of which have special relevance for PD. Based on published clinical studies in PD, there is now a clearer emerging picture of the ways in which 7T MRI is beneficial for image quality and research. However, more work is needed to show whether these improvements in image quality will benefit clinical decision making. One area in which 7T MRI has shown tangible benefits to clinical decision making is in DBS surgical planning, but for diagnosis, differential diagnosis, subtyping and measurement of treatment response, further evidence is required in larger and earlier-stage cohorts. Moreover, any clinical benefits need to be great enough to justify the additional costs.

Acknowledgments

We thank Olivier Mougin (Sir Peter Mansfield Imaging

Centre, University of Nottingham, Nottingham, UK) for providing the 7T MRI images used in Figure 4.

Funding: None.

Footnote

Reporting Checklist: The authors have completed the Narrative Review reporting checklist. Available at <https://qims.amegroups.com/article/view/10.21037/qims-23-509/rc>

Conflicts of Interest: All authors have completed the ICMJE uniform disclosure form (available at <https://qims.amegroups.com/article/view/10.21037/qims-23-509/coif>). EKT reports receiving honorarium from Wiley and Eisai for editorial and academic activities. NH reports that he is a co-founder of Surgical Information Sciences, Inc., and reports grant support from the National Institutes of Health (Nos. R01 NS081118, R01 NS113746, S10 OD025256, P41EB027061, P50 NS123109). DPA reports grant support received to undertake research in Parkinson's disease from MJFF, Weston Brain Institute, NIHR, MRC, and Biogen. The other authors have no conflicts of interest to declare.

Ethical Statement: The authors are accountable for all aspects of the work in ensuring that questions related to the accuracy or integrity of any part of the work are appropriately investigated and resolved.

Open Access Statement: This is an Open Access article distributed in accordance with the Creative Commons Attribution-NonCommercial-NoDerivs 4.0 International License (CC BY-NC-ND 4.0), which permits the non-commercial replication and distribution of the article with the strict proviso that no changes or edits are made and the original work is properly cited (including links to both the formal publication through the relevant DOI and the license). See: <https://creativecommons.org/licenses/by-nc-nd/4.0/>.

References

1. Vaughan JT, Garwood M, Collins CM, Liu W, DelaBarre L, Adriany G, Andersen P, Merkle H, Goebel R, Smith MB, Ugurbil K. 7T vs. 4T: RF power, homogeneity, and signal-to-noise comparison in head images. *Magn Reson Med* 2001;46:24-30.
2. Yacoub E, Harel N, Ugurbil K. High-field fMRI unveils orientation columns in humans. *Proc Natl Acad Sci U S A* 2008;105:10607-12.

3. Balchandani P, Naidich TP. Ultra-High-Field MR Neuroimaging. *AJNR Am J Neuroradiol* 2015;36:1204-15.
4. van der Kolk AG, Hendrikse J, Zwanenburg JJ, Visser F, Luijten PR. Clinical applications of 7 T MRI in the brain. *Eur J Radiol* 2013;82:708-18.
5. Global, regional, and national burden of Parkinson's disease, 1990-2016: a systematic analysis for the Global Burden of Disease Study 2016. *Lancet Neurol* 2018;17:939-53.
6. Lee H, Baek SY, Kim EJ, Huh GY, Lee JH, Cho H. MRI T(2) and T(2)* relaxometry to visualize neuromelanin in the dorsal substantia nigra pars compacta. *Neuroimage* 2020;211:116625.
7. Rua C, O'Callaghan C, Ye R, Hezemans FH, Passamonti L, Jones PS, Williams GB, Rodgers CT, Rowe JB. Substantia nigra ferric overload and neuromelanin loss in Parkinson's disease measured with 7T MRI. *medRxiv* 2021. doi: <https://doi.org/10.1101/2021.04.13.21255416>.
8. Poston KL, Ua Cruadhlaioich MAI, Santoso LF, Bernstein JD, Liu T, Wang Y, Rutt B, Kerchner GA, Zeineh MM. Substantia Nigra Volume Dissociates Bradykinesia and Rigidity from Tremor in Parkinson's Disease: A 7 Tesla Imaging Study. *J Parkinsons Dis* 2020;10:591-604.
9. Lehericy S, Vaillancourt DE, Seppi K, Monchi O, Rektorova I, Antonini A, McKeown MJ, Masellis M, Berg D, Rowe JB, Lewis SJG, Williams-Gray CH, Tessitore A, Siebner HR, on behalf of the International Parkinson and Movement Disorder Society (IPMDS)-Neuroimaging Study Group. The role of high-field magnetic resonance imaging in parkinsonian disorders: Pushing the boundaries forward. *Mov Disord* 2017;32:510-25.
10. Düzel E, Costagli M, Donatelli G, Speck O, Cosottini M. Studying Alzheimer disease, Parkinson disease, and amyotrophic lateral sclerosis with 7-T magnetic resonance. *Eur Radiol Exp* 2021;5:36.
11. Schwarz ST, Afzal M, Morgan PS, Bajaj N, Gowland PA, Auer DP. The 'swallow tail' appearance of the healthy nigrosome - a new accurate test of Parkinson's disease: a case-control and retrospective cross-sectional MRI study at 3T. *PLoS One* 2014;9:e93814.
12. Uğurbil K. Imaging at ultrahigh magnetic fields: History, challenges, and solutions. *Neuroimage* 2018;168:7-32.
13. Webb AG, Van de Moortele PF. The technological future of 7T MRI hardware. *NMR Biomed* 2016;29:1305-15.
14. Vachha B, Huang SY. MRI with ultrahigh field strength and high-performance gradients: challenges and opportunities for clinical neuroimaging at 7 T and beyond. *Eur Radiol Exp* 2021;5:35.
15. Lehericy S, Bardin E, Poupon C, Vidailhet M, François C. 7 Tesla magnetic resonance imaging: a closer look at substantia nigra anatomy in Parkinson's disease. *Mov Disord* 2014;29:1574-81.
16. Gramsch C, Reuter I, Kraff O, Quick HH, Tanislav C, Roessler F, Deuschl C, Forsting M, Schlamann M. Nigrosome 1 visibility at susceptibility weighted 7T MRI-A dependable diagnostic marker for Parkinson's disease or merely an inconsistent, age-dependent imaging finding? *PLoS One* 2017;12:e0185489.
17. Fagan AJ, Amrami KK, Welker KM, Frick MA, Felmlee JP, Watson RE Jr. Magnetic Resonance Safety in the 7T Environment. *Magn Reson Imaging Clin N Am* 2020;28:573-82.
18. Hoff MN, McKinney A 4th, Shellock FG, Rassner U, Gilk T, Watson RE Jr, Greenberg TD, Froelich J, Kanal E. Safety Considerations of 7-T MRI in Clinical Practice. *Radiology* 2019;292:509-18.
19. Duchin Y, Shamir RR, Patriat R, Kim J, Vitek JL, Sapiro G, Harel N. Patient-specific anatomical model for deep brain stimulation based on 7 Tesla MRI. *PLoS One* 2018;13:e0201469.
20. Sung YH, Kim JS, Yoo SW, Shin NY, Nam Y, Ahn TB, et al. A prospective multi-centre study of susceptibility map-weighted MRI for the diagnosis of neurodegenerative parkinsonism. *Eur Radiol* 2022;32:3597-608.
21. Liu X, Wang N, Chen C, Wu PY, Piao S, Geng D, Li Y. Swallow tail sign on susceptibility map-weighted imaging (SMWI) for disease diagnosing and severity evaluating in parkinsonism. *Acta Radiol* 2021;62:234-42.
22. Schwarz ST, Mougín O, Xing Y, Blazejewska A, Bajaj N, Auer DP, Gowland P. Parkinson's disease related signal change in the nigrosomes 1-5 and the substantia nigra using T2* weighted 7T MRI. *Neuroimage Clin* 2018;19:683-9.
23. Patriat R, Niederer J, Kaplan J, Amundsen Huffmaster S, Petrucci M, Eberly L, Harel N, MacKinnon C. Morphological changes in the subthalamic nucleus of people with mild-to-moderate Parkinson's disease: a 7T MRI study. *Sci Rep* 2020;10:8785.
24. Gao LL, Wu T. The study of brain functional connectivity in Parkinson's disease. *Transl Neurodegener* 2016;5:18.
25. Atkinson-Clement C, Pinto S, Eusebio A, Coulon O. Diffusion tensor imaging in Parkinson's disease: Review and meta-analysis. *Neuroimage Clin* 2017;16:98-110.
26. Lotfipour AK, Wharton S, Schwarz ST, Gontu V, Schäfer A, Peters AM, Bowtell RW, Auer DP, Gowland PA, Bajaj NP. High resolution magnetic susceptibility mapping of

- the substantia nigra in Parkinson's disease. *J Magn Reson Imaging* 2012;35:48-55.
27. Lee H, Baek SY, Chun SY, Lee JH, Cho H. Specific visualization of neuromelanin-iron complex and ferric iron in the human post-mortem substantia nigra using MR relaxometry at 7T. *Neuroimage* 2018;172:874-85.
 28. Isaacs BR, Mulder MJ, Groot JM, van Berendonk N, Lute N, Bazin PL, Forstmann BU, Alkemade A. 3 versus 7 Tesla magnetic resonance imaging for parcellations of subcortical brain structures in clinical settings. *PLoS One* 2020;15:e0236208.
 29. Schrock LE, Patriat R, Goftari M, Kim J, Johnson MD, Harel N, Vitek JL. 7T MRI and Computational Modeling Supports a Critical Role of Lead Location in Determining Outcomes for Deep Brain Stimulation: A Case Report. *Front Hum Neurosci* 2021;15:631778.
 30. Alkemade A, de Hollander G, Keuken MC, Schäfer A, Ott DVM, Schwarz J, Weise D, Kotz SA, Forstmann BU. Comparison of T2*-weighted and QSM contrasts in Parkinson's disease to visualize the STN with MRI. *PLoS One* 2017;12:e0176130.
 31. Blazejewska AI, Schwarz ST, Pitiot A, Stephenson MC, Lowe J, Bajaj N, Bowtell RW, Auer DP, Gowland PA. Visualization of nigrosome 1 and its loss in PD: pathoanatomical correlation and in vivo 7 T MRI. *Neurology* 2013;81:534-40.
 32. Cosottini M, Frosini D, Pesaresi I, Costagli M, Biagi L, Ceravolo R, Bonuccelli U, Tosetti M. MR imaging of the substantia nigra at 7 T enables diagnosis of Parkinson disease. *Radiology* 2014;271:831-8.
 33. Eapen M, Zald DH, Gatenby JC, Ding Z, Gore JC. Using high-resolution MR imaging at 7T to evaluate the anatomy of the midbrain dopaminergic system. *AJNR Am J Neuroradiol* 2011;32:688-94.
 34. Cosottini M, Frosini D, Pesaresi I, Donatelli G, Cecchi P, Costagli M, Biagi L, Ceravolo R, Bonuccelli U, Tosetti M. Comparison of 3T and 7T susceptibility-weighted angiography of the substantia nigra in diagnosing Parkinson disease. *AJNR Am J Neuroradiol* 2015;36:461-6.
 35. Abosch A, Yacoub E, Ugurbil K, Harel N. An assessment of current brain targets for deep brain stimulation surgery with susceptibility-weighted imaging at 7 tesla. *Neurosurgery* 2010;67:1745-56; discussion 1756.
 36. Priovoulos N, Jacobs HIL, Ivanov D, Uludağ K, Verhey FRJ, Poser BA. High-resolution in vivo imaging of human locus coeruleus by magnetization transfer MRI at 3T and 7T. *Neuroimage* 2018;168:427-36.
 37. Ye R, O'Callaghan C, Rua C, Hezemans FH, Holland N, Malpetti M, Jones PS, Barker RA, Williams-Gray CH, Robbins TW, Passamonti L, Rowe J. Locus Coeruleus Integrity from 7T MRI Relates to Apathy and Cognition in Parkinsonian Disorders. *Mov Disord* 2022;37:1663-72.
 38. Tona KD, van Osch MJP, Nieuwenhuis S, Keuken MC. Quantifying the contrast of the human locus coeruleus in vivo at 7 Tesla MRI. *PLoS One* 2019;14:e0209842.
 39. Liebe T, Kaufmann J, Hämmerer D, Betts M, Walter M. In vivo tractography of human locus coeruleus-relation to 7T resting state fMRI, psychological measures and single subject validity. *Mol Psychiatry* 2022;27:4984-93.
 40. Schmidt MA, Engelhorn T, Marxreiter F, Winkler J, Lang S, Kloska S, Goelitz P, Doerfler A. Ultra high-field SWI of the substantia nigra at 7T: reliability and consistency of the swallow-tail sign. *BMC Neurol* 2017;17:194.
 41. Lenglet C, Abosch A, Yacoub E, De Martino F, Sapiro G, Harel N. Comprehensive in vivo mapping of the human basal ganglia and thalamic connectome in individuals using 7T MRI. *PLoS One* 2012;7:e29153.
 42. Cho ZH, Oh SH, Kim JM, Park SY, Kwon DH, Jeong HJ, Kim YB, Chi JG, Park CW, Huston J 3rd, Lee KH, Jeon BS. Direct visualization of Parkinson's disease by in vivo human brain imaging using 7.0T magnetic resonance imaging. *Mov Disord* 2011;26:713-8.
 43. Kwon DH, Kim JM, Oh SH, Jeong HJ, Park SY, Oh ES, Chi JG, Kim YB, Jeon BS, Cho ZH. Seven-Tesla magnetic resonance images of the substantia nigra in Parkinson disease. *Ann Neurol* 2012;71:267-77.
 44. Plantinga BR, Temel Y, Duchin Y, Uludağ K, Patriat R, Roebroek A, Kuijf M, Jahanshahi A, Ter Haar Romenij B, Vitek J, Harel N. Individualized parcellation of the subthalamic nucleus in patients with Parkinson's disease with 7T MRI. *Neuroimage* 2018;168:403-11.
 45. Oh BH, Moon HC, Kim A, Kim HJ, Cheong CJ, Park YS. Prefrontal and hippocampal atrophy using 7-tesla magnetic resonance imaging in patients with Parkinson's disease. *Acta Radiol Open* 2021;10:2058460120988097.
 46. Filippi M, Sarasso E, Piramide N, Stojkovic T, Stankovic I, Basaia S, Fontana A, Tomic A, Markovic V, Stefanova E, Kostic VS, Agosta F. Progressive brain atrophy and clinical evolution in Parkinson's disease. *Neuroimage Clin* 2020;28:102374.
 47. Vitek JL, Patriat R, Ingham L, Reich MM, Volkmann J, Harel N. Lead location as a determinant of motor benefit in subthalamic nucleus deep brain stimulation for Parkinson's disease. *Front Neurosci* 2022;16:1010253.
 48. Husch A, Petersen MV, Gemmar P, Goncalves J, Sunde N, Hertel F. Post-operative deep brain stimulation assessment:

- Automatic data integration and report generation. *Brain Stimul* 2018;11:863-6.
49. Patriat R, Cooper SE, Duchin Y, Niederer J, Lenglet C, Aman J, Park MC, Vitek JL, Harel N. Individualized tractography-based parcellation of the globus pallidus pars interna using 7T MRI in movement disorder patients prior to DBS surgery. *Neuroimage* 2018;178:198-209.
 50. Bianciardi M, Strong C, Toschi N, Edlow BL, Fischl B, Brown EN, Rosen BR, Wald LL. A probabilistic template of human mesopontine tegmental nuclei from in vivo 7T MRI. *Neuroimage* 2018;170:222-30.
 51. Milchenko M, Norris SA, Poston K, Campbell MC, Ushe M, Perlmutter JS, Snyder AZ. 7T MRI subthalamic nucleus atlas for use with 3T MRI. *J Med Imaging (Bellingham)* 2018;5:015002.
 52. Ye R, Rua C, O'Callaghan C, Jones PS, Hezemans FH, Kaalund SS, Tsvetanov KA, Rodgers CT, Williams G, Passamonti L, Rowe JB. An in vivo probabilistic atlas of the human locus coeruleus at ultra-high field. *Neuroimage* 2021;225:117487.
 53. Callaghan F, Maller JJ, Welton T, Middione MJ, Shankaranarayanan A, Grieve SM. Toward personalised diffusion MRI in psychiatry: improved delineation of fibre bundles with the highest-ever angular resolution in vivo tractography. *Transl Psychiatry* 2018;8:91.
 54. Wu X, Auerbach EJ, Vu AT, Moeller S, Lenglet C, Schmitter S, Van de Moortele PF, Yacoub E, Uğurbil K. High-resolution whole-brain diffusion MRI at 7T using radiofrequency parallel transmission. *Magn Reson Med* 2018;80:1857-70.
 55. Frosini D, Ceravolo R, Tosetti M, Bonuccelli U, Cosottini M. Nigral involvement in atypical parkinsonisms: evidence from a pilot study with ultra-high field MRI. *J Neural Transm (Vienna)* 2016;123:509-13.
 56. Kim JM, Jeong HJ, Bae YJ, Park SY, Kim E, Kang SY, Oh ES, Kim KJ, Jeon B, Kim SE, Cho ZH, Kim YB. Loss of substantia nigra hyperintensity on 7 Tesla MRI of Parkinson's disease, multiple system atrophy, and progressive supranuclear palsy. *Parkinsonism Relat Disord* 2016;26:47-54.
 57. Frosini D, Cosottini M, Donatelli G, Costagli M, Biagi L, Pacchetti C, Terzaghi M, Cortelli P, Arnaldi D, Bonanni E, Tosetti M, Bonuccelli U, Ceravolo R. Seven tesla MRI of the substantia nigra in patients with rapid eye movement sleep behavior disorder. *Parkinsonism Relat Disord* 2017;43:105-9.
 58. Shin DH, Heo H, Song S, Shin NY, Nam Y, Yoo SW, Kim JS, Yoon JH, Lee SH, Sung YH, Kim EY. Automated assessment of the substantia nigra on susceptibility map-weighted imaging using deep convolutional neural networks for diagnosis of Idiopathic Parkinson's disease. *Parkinsonism Relat Disord* 2021;85:84-90.
 59. Sung YH, Noh Y, Kim EY. Early-stage Parkinson's disease: Abnormal nigrosome 1 and 2 revealed by a voxelwise analysis of neuromelanin-sensitive MRI. *Hum Brain Mapp* 2021;42:2823-32.
 60. Sung YH, Lee J, Nam Y, Shin HG, Noh Y, Shin DH, Kim EY. Differential involvement of nigral subregions in idiopathic parkinson's disease. *Hum Brain Mapp* 2018;39:542-53.
 61. Wolters AF, Heijmans M, Michielse S, Leentjens AFG, Postma AA, Jansen JFA, Ivanov D, Duits AA, Temel Y, Kuijff ML. The TRACK-PD study: protocol of a longitudinal ultra-high field imaging study in Parkinson's disease. *BMC Neurol* 2020;20:292.

Cite this article as: Welton T, Hartono S, Shih YC, Schwarz ST, Xing Y, Tan EK, Auer DP, Harel N, Chan LL. Ultra-high-field 7T MRI in Parkinson's disease: ready for clinical use?—a narrative review. *Quant Imaging Med Surg* 2023;13(11):7607-7620. doi: 10.21037/qims-23-509